Photosensitive Glass Modification Based on Infrared CO_2-laser Irradiation

V. Veiko[1], E. Ageev[1], M. Sergeev[1], A. Petrov[1], M. Doubenskaia[2]

[1] *National Research University of Information Technologies, Mechanics and Optics, Kronverkskiy pr., 49, 197101, Saint Petersburg, Russia*
[2] *Université de Lyon, Ecole Nationale d'Ingénieurs de Saint Etienne (ENISE), DIPI Laboratory, 58 rue Jean Parot, 42023 Saint-Étienne Cedex 2, France*
E-mail: veiko@lastech.ifmo.ru

The action of laser radiation with wavelength λ = 10.6 μm causes substantial phase and structural changes in photosensitive glass as a consequence of the processes of induced crystallization and secondary amorphisation, which are reversible. Obtained polycrystalline phases were investigated by means of X-ray diffractometry (XRD), optical spectroscopy and Raman scattering spectroscopy. CO_2-laser exposure could replace traditional heating in furnace during crystallization procedure effectively reducing total processing time.

DOI:10.2961/jlmn.2013.02.0007

Keywords: CO_2-laser, photosensitive glass, induced crystallization, secondary amorphisation.

1. Introduction

Particular interest for phase-changing materials is caused by the fact that it has rather wide prospects of implementation for microanalytical systems, nanosatellites and etc. [1]-[4] whilst its treatment technology leading to crystallization is highly complex. Traditional technology consists from three steps including UV photoactivation (10-15 minutes) and two stages of heat treatment with total duration more than 3 hours with subsequent inertial cooling which lasts for 3-4 hours [5]. In such way writing process becomes indirect and highly time-consuming. For example, in case of Foturan™ photosensitive glass after a first photochemical stage colloidal silver clusters with submicrometer dimensions appear. It leads to light yellow coloration of material without absorbance spectrum considerable changes. After a second stage there is a first heat treatment at 400-500°C, lithium metasilicate (LMS) Li_2SiO_3 crystalline phase precipitates onto silver colloidal particles [6]. Polycrystalline phase growth and formation of all new material properties (including drastic fall of optical transparency due to absorption and scattering of visible light) are the results of third stage which is a second heat treatment at 550-650°C.

Our previous studies [7], [8], carried out on titaniferous glass-ceramics ST-50-1, in contrast demonstrated a one stage amorphisation and crystallization (it is quick about tens of seconds). These experiments show that local (focused to the spot with 100 μm diameter) action of CO_2-laser with power density $5x10^5$ W/m^2 results in material amorphisation. Next irradiation with lower power densities 10^5 W/m^2 (hence with lower heating and cooling rates) offers a possibility of its one-stage reverse crystallization to original material state. This results was explained by CO_2-laser (λ = 10.6 μm) radiation absorption on silica-oxygen bonds (with quantum energy $h\nu$ ~ 0.12 eV) corresponding to its characteristic absorption with subsequent nonequilibrium crystallization from non-ideal laser-produced melt onto density fluctuations generated by strong thermal gradient at irradiated areas.

Going back to photosensitive glass it should be noted that crystalline structures arising there under exposure of different laser sources in a wide range from CW UV (He-Cd laser) to pulses of nanosecond (N_2-laser) or even picosecond [9] or femtosecond [10] width and CW IR CO_2-laser [11] are almost identical (so far as it could be defined from optical spectra comparison).

CO_2-laser action on Foturan™ was studied in the paper [12], where the local crystallization and secondary amorphisation of this glass were shown

In this paper more detailed experimental investigation regarding crystallization of photosensitive glasses under CO_2-laser are presented. The rates of heating –cooling and crystallization – amorphisation are measured and the properties of resulting phases are considered.

2. Photosensitive glass laser modification procedure

The following experiments were carried out to reveal the influence of various factors on the crystallization process:

1. The basic experiment including traditional steps: CW UV He-Cd-laser irradiation and standard double-stage heat treatment [13] (UV+T). In [14] it was shown for photosensitive glass that heating by means of CO_2-laser replaces heat treatment in a furnace and results in formation of crystal structures which, however, haven't been investigated completely;
2. The next step was the CW UV He-Cd-laser irradiation (or, for example, pulse N_2-laser) followed by CO_2-laser action instead of heat treatment in a furnace (UV+CO2);
3. The subsequent development of the previous experiment, which was positive in sense of crystal phase formation also, became CO_2-laser irradiation only without the use of UV and heat treatment (CO2);
4. The next experiment was the control and combined CO_2-laser action and traditional heat treatment (CO2+T).

The general layout of the experiments for crystallization process is presented in Fig. 1.

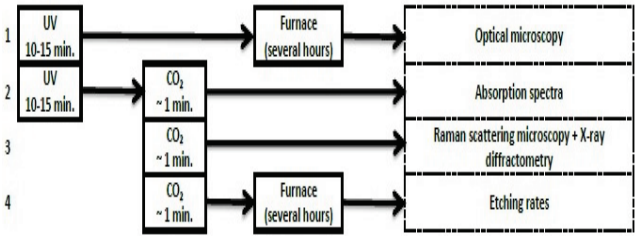

Fig. 1. The overall layout of the experiments for crystallization process: methods of crystallization and comparison of a nascent crystal phases. The time between consequent processing steps could vary from minutes to days. The penetration depth of radiation at $\lambda = 10.6$ μm in the glass is about 1.25 μm.

Each of the processing regimes mentioned above leads to formation of polycrystalline (glass ceramic) nontransparent structure. All experiments on crystallization were followed by CO_2-laser induced amorphisation. All resulting structures, both polycrystalline and amorphous, were investigated under a microscope, as well as by the X-ray diffractometry (XRD), optical spectroscopy and Raman scattering spectroscopy. FS-1 glass material composition was a conventional: SiO_2 – 79, Li_2O – 9, K_2O – 2.5, Al_2O_3 – 7.5, Ag_2O – 0.002, Ce_2O_3 – 0.02 (wt. %). Samples were prepared in the form of plane plates with thickness about 1 mm.

In the all processing regimes CO_2-laser exposure parameters were the same: the power density is $q \sim 3.0 \times 10^5$ W/m^2, and the exposure duration was 40-240 s. In the all cases a preheating was necessary to avoid cracking of the samples, and after temperature reaches this value the general processing begins. In our experiments a preheating was realized by the same CO_2-laser by special low intensity channel, the preheating time was about 20-40 s and the preheating temperature T_0 is about 400ºC. In these conditions the measured value of temperature T_{cr} at which crystallization processes begin at the surface was T_{cr} = 950-1150ºC. The melting temperature for the center of laser spot was estimated from the known power density q and the exposure duration τ with the use of formula [15]:

$$T = (2/\sqrt{\pi}) \cdot q(1-R)\sqrt{a\tau}/k + T_0 \qquad (1)$$

where a and k – the thermal diffusivity and the heat conductivity, for FS-1 their values are $a = 5 \cdot 10^{-7}$ m^2/s, k = 1.45 W/m·K, R is the reflectivity and appears equal to 1200°C which is in acceptable correspondence with measured from the experiments as an average for the spot about 5 mm (Fig. 2, a).

The laser-induced amorphisation regime was also based on CW CO_2-laser irradiation. The measured value of temperature at the beginning of amorphisation process was T_{am} = 1200-1300°C, while the threshold power density $q \sim 1.0 \times 10^7$ W/m^2. The preheating temperature is the same as for crystallization procedure. The heating time by laser is 70-100 s.

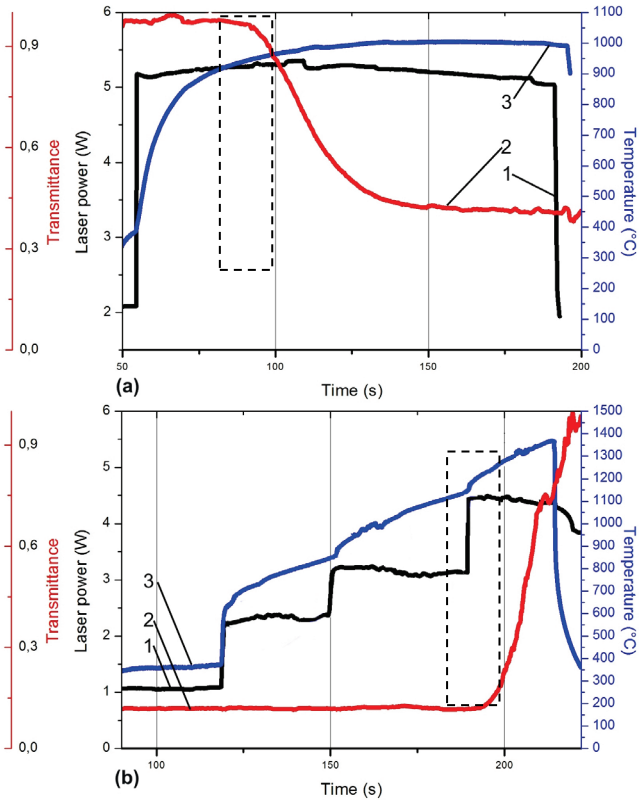

Fig. 2. The phase transition kinetics during exposure of FS-1 glass by CO_2 –laser: a) crystallization, b) secondary amorphisation: 1 – CO_2-laser power (incremental increase, spot diameters were 5 and 0.5 mm for crystallization and amorphisation processes, correspondingly), 2 – the alteration of probe laser radiation transmittance in the middle of irradiated area, 3 – the temperature of material in the middle of irradiated area. The rectangle indicates the area where crystallization or amorphisation starts, correspondingly.

On Fig. 2 one can see the phase transition kinetics during exposure of FS-1 glass by CO_2–laser for crystallization (method 3 according to Fig. 1) and for secondary amorphisation of the same sample (Fig. 2 a and b). Heating rate during CO_2-laser induced crystallization measured from Fig.2, a is equal to $V_{heat.} \sim$ 30-80 K/s and corresponding crystallization front rate is in the range 15-25 μm/s. As for cooling rates during CO_2-laser induced secondary amorphisation it is also can be seen at Fig.2, b and it is equal to $V_{cool.} \sim$ 100-150 K/s and corresponding amorphisation front rate is about 20 μm/s. Greater values of heating/cooling rates result in cracks formation.

3. Laser-induced modification results

The external view of FS-1 material before and after photo-thermo-induced processing is shown on Fig. 3.

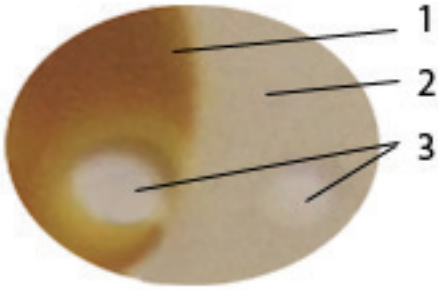

Fig. 3. FS-1 appearance before and after laser-induced crystallization and secondary amorphisation [12]: 1 – after the UV irradiation and heat treatment; 2 – the original amorphous FS-1 glass; 3- after the secondary amorphisation.

The next step of our studies was the FS-1 amorphisation by CO_2-laser IR radiation. After such treatment the yellow coloration and the strong light scattering disappear. Irradiated area becomes transparent for visible light (Fig. 3). In other words IR laser-induced treatment results in the transition to the initial glass.

In the case of photo-thermo-induced crystallization (UV+T) the given mechanism is well-known (looks for example [16] and is based on the photochemical reaction of cerium ions ionization by UV radiation with the generation of free electrons, the deoxidation of silver atoms and the subsequent formation of crystallization centers, where on thermal growth of the crystalline phase occurs (clustered crystallization).

It seems the mechanism of single step IR laser-induced crystallization is the following. Nonequilibrium, non-stationary and nonhomogeneous material heating occurs because of fundamental absorption at vibrational-rotational transitions of silicon-oxygen bonds and results in lattice temperature increase. Temperature fields with strong thermal gradient (~500 K/s) appear and cause nonequilibrium crystallization (with the limited diffusion and drift of ions) at density fluctuations. Microstructures of nascent crystals have a strong dependence on time and heating-cooling rates according to the LCDV (liquid–deformed-crystal-vacancy) hypothesis [17].

The overall forms (Fig. 3) as well as identical absorption spectra are the experimental confirmation of mechanism described above: the spectrum of glass after secondary amorphisation (Fig. 4, b.) gives an evidence of FS-1 original structure recovery with UV photosensitivity restoration having an absorption peak at λ = 313 nm as a consequence of regeneration of Ce^{3+} ions and it can be seen that the absorption band of colloidal silver (λ = 420 nm) completely disappears. It is possible to name such transition as the reverse structural modification, since the initial glass becomes a polycrystalline material and then it becomes a secondary glass with spectral characteristics closed to initial, and such transitions could be repetitive.

3.1. Material properties change after processing

Optical transparency.

Radical changes in the optical transparency of the material can be observed by the naked eye in the form of the simultaneous (with a material irradiation by a laser beam) appearance of an opaque region in the transparent material. Absorbance spectra of areas crystallized under different methods are presented on Fig. 4, a. Predictably material absorption characteristics have changed after laser action.

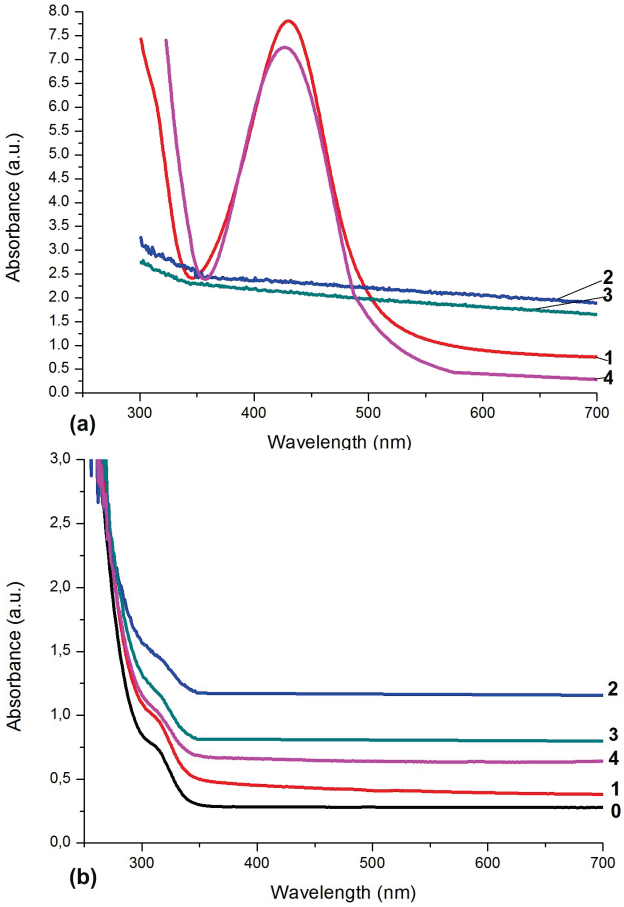

Fig. 4. Absorption spectra of photosensitive glass:
a) after the crystallization by different methods: 1 – the UV action together with heat treatment (UV+T); 2 – the CO_2-laser action only (CO2); 3 – the UV together with the CO_2-laser action (UV+CO2); 4 – the CO_2-laser action together with the heat treatment (CO2+T);
b) after the secondary amorphisation by the CO_2-laser action, corresponding to different crystallization methods (1-4) and the FS-1 virgin glass (0).

Absorbance spectra of material regions after secondary amorphisation are shown in Fig. 4, b. The comparison of spectra of secondary amorphisated areas with virgin glass spectrum allows one to tell, that after the amorphisation the material almost completely restores its spectral properties.

Etching rates.

Etching rates of the material after the crystallization and after the secondary amorphisation in a 5 mass% solution of hydrofluoric acid were measured [18] and presented in Table 1. After the secondary amorphisation they are in a range from 0,6±0,1 μm/min to 1,2±0,2 μm/min that give an evidence of returning to an initial material condition as well, because the virgin glass etching rate was measured as 0.8±0.2 μm/min.

Table 1. Etching rates of various crystalline and secondary amorphisated phases.

Processing protocol		1 (UV+T)	2 (UV+CO_2)	3 (CO_2)	4 (CO_2+T)
Mean etching rate *dh/dt*, μm/min	after crystalli-zation	8.1±0.8	3.7±0.1	3.3±0.1	9.3±0.8
	after secondary amorphi-sation	1.0±0.3	0.6±0.1	0.6±0.1	1.2±0.2

Note. Original material FS-1, *dh/dt* = 0.8±0.2 μm/min.

Identification of obtained crystalline phase.

Raman scattering spectroscopy spectra of samples crystallized according to (UV+T) and (CO2) protocols are shown in Fig. 5, a and b, correspondingly. Spectra were measured on micro-Raman spectrometer «in-Via Renishaw» in the back scattering geometry, equipped with a multichannel CCD camera cooled to -70 °C. An ion argon laser with wavelength 514.5 nm was used as a spectrum excitation source. The light was focused on the sample by 50^x Leica objective with NA = 0.78, at this focal spot on the sample surface was ~ 2 μm in diameter.

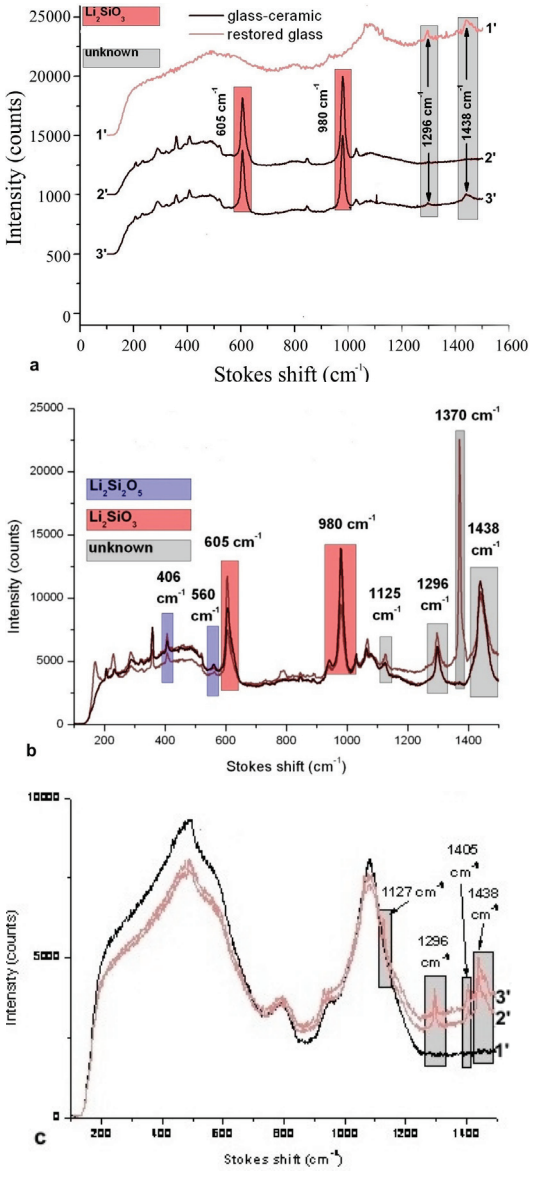

Fig. 5. Raman scattering spectra of FS-1 glass samples:
a) – crystallized using (UV+T) method: 1' – glass after secondary amorphisation, 2' and 3' – 2 different points on sample surface after crystallization;
b) - crystallized using (CO2) method: 3 different points on sample surface after crystallization;
c) - after crystallization using (CO2) method and secondary amorphisation: 1' - virgin glass, 2'and 3' - glass after secondary amorphisation.

Results obtained for two different points on the surface of a single sample indicate, that the arising crystalline phase of the LMS is identical for both represented crystallization methods. If there is no heat treatment stage in a furnace, the crystalline phase of the lithium disilicate (LDS) also appears. There are strong peaks centered at 605 cm^{-1} and 980 sm^{-1}, corresponding to LMS (Li_2SiO_3) and peaks centered at 406 cm^{-1}, 560 cm^{-1} and 1125 cm^{-1} belong to LDS ($Li_2Si_2O_5$). There are also peaks at 1127 cm^{-1}, 1296 cm^{-1}, 1370 cm^{-1} and 1438 cm^{-1} for unknown compound.

XRD results were obtained by the X-ray diffractometer «Rigaku Ultima IV». Collected XRD patterns were analyzed in PDXL software using ICDD PDF-2 database of diffractograms. According to XRD results (Fig. 6) nascent crystalline phase for all methods is LMS. It seems that absence of LDS peaks on the X-ray diffractogram indicates a trace amount of this phase.

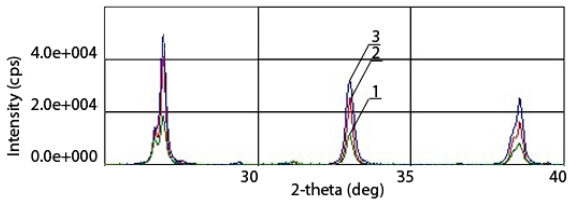

Fig. 6. XRD pattern of FS-1 glass samples crystallized using different methods: 1 (green line) – the UV action together with heat treatment (UV+T), 2 (red line) – the CO_2-laser action only (CO2), 3 (blue line) – the CO_2-laser action together with the heat treatment (CO2+T).

The Raman scattering spectra in Fig. 5, c is obtained from a sample crystallized using the (CO2) method. Taking into account secondary amorphisation results presented in Fig. 5, a it can apparently be said that silver crystallization centers have a different nature in samples that have not been subjected to preliminary UV action and those that have been subjected to UV radiation. The process by which this region is formed has a purely thermophysical character in the former case, whereas "traditional" silver-crystallization centers are formed in samples preirradiated with UV radiation, and the process itself has a photochemical nature. It should be noted that Raman scattering spectrum of material after crystallization using (CO2) method and after secondary amorphisation demonstrates that there are bands of unknown compound which are generated during a crystallization and do not disappear in a glass after the secondary amorphisation. This question needs additional study.

4. Discussion

These results give an opportunity to suggest that using different crystallization methods causes two different kinds of structures to appear. According to Fig. 4, a absorbance spectra could be divided into two groups, the first is from protocols 1 (UV+T) and 4 (CO_2+T) and the second is from protocols 2 (UV+CO_2) and 3 (CO_2). The same separation can be made on the basis of data on the etching rates from Table 1. Based on these results a conclusion can be drawn that different processing conditions leads to appearance of enough stable, but various from each other types of structures.

It is known the crystallization process consists of two stages: 1) nucleation centers nascence and 2) the growth of the crystalline phase. It is possible to note that the distinction between the obtained crystalline structures corresponds to a difference in a way of heat treatment. With prolonged heat treatment following for UV or IR irradiation there are identical crystalline structure types. It is interesting to note that the method of creating crystallization centers has no matter in this case, if it is the photoinduced generation under UV irradiation or spontaneous following local heating by CO_2-laser radiation.

The reverse situation is observed when instead of equilibrium heat treatment a short, non-stationary and nonequilibrium CO_2-laser action is applied. Such action results in the formation of other structures that differ both externally and in their absorption spectra, but at the same time are similar to each other whereas one of them is created by UV action with subsequent IR irradiation and the other only by IR irradiation and both without heat treatment in a furnace.

This distinction between two types of structures can become clearer if one considers the second stage of crystallization; it is the growth of the crystalline phase including diffusion to the nucleation centers from the surrounding material. In case of long isothermal heating in a furnace all required ions arrive to nucleation centers with no limitations until an equilibrium crystalline phase appears at the given temperature (in our case it is LMS). In a case of short-term CO_2-laser action, the heating process is dynamic and takes a very short (relative to heating in a furnace) time. The diffusion length $l_{dif}=\sqrt{d\tau}$ is very small. For glass with diffusion coefficient $d \sim 10^{-13}$ m^2/s and τ=1 s, it is $l_{\text{dif}} \sim 10^{-7}$ m < 1 μm. Therefore in case of short non-stationary laser heating in accordance with the Ostwald rule the intermediate metastable crystalline phases [17] are formed that differ from equilibrium phases but have a high degree of repeatability under CO_2-laser exposure. For our investigation they correspond to a LMS and LDS mixture.

According to the data of Raman scattering spectroscopy and XRD measurements the resulting crystalline phase also corresponds to LMS for samples obtained with heat treatment in a furnace. In this case, according to the Raman-scattering data in samples that were processed with no prolonged thermal action, LDS is present along with the LMS.

All obtained crystalline structures are highly reversible and are transferable to the amorphous state that is virtually indistinguishable from the original glass.

As for amorphisation to speculate a mechanism of the secondary amorphisation it is necessary to take into account two facts: 1) the laser heated zone $l_{heat}=\sqrt{a\tau}$ at the exposure time (20–100 s) is 5–7 mm which is much more than the thickness of the sample and the heating time is enough to produce thermodynamic equilibrium melt, and 2) all optical properties of the initial glass are restored in the secondary one. Based on these facts the tentative mechanism of the secondary amorphisation could be proposed as the following: a) melting of Li_2SiO_3 microcrystals with interruption and release of long-range order bonds in liquid melt $Li_2O-SiO_2\,(\text{crystal}) \xrightarrow{melting} Li_2O-SiO_2\,(\text{liquid melt})$; b) dissolution of silver clusters in the liquid melt with interruption of one weak external bond and valence electrons release $(Ag)_n \rightarrow nAg^+ + ne^-$, and capture of released electrons by Ce^{4+} ions with their partial reduction $Ce^{4+} + e^- \rightarrow Ce^{3+}$ and with restoration of optical properties.

4. Conclusions

1. The capability of the IR CO_2-laser radiation with wavelength 10.6 μm to induce the local crystallization (C) of photosensitive lithium-alumosilicate glass FS-1 has been proved and experimentally confirmed. The IR action leads to nucleation centers formation based on density fluctuations with subsequent growth of crystals with limited diffusion and drift of elements causing "freezing" of any given metastable state of liquid melt of a basic material due to high rates of heating-cooling.

2. It is possible to have secondary amorphisation (A) of the structure, obtained by the local laser crystallization. Under laser heating it has such mechanism: there are disordering and melting of polycrystals, the dissociation of silver molecules with separation of valence electrons and their subsequent trapping by Ce^{4+} ions and formation of the amorphous phase of the glass.

3. Repeated reversible changes of the FS-1 – phase-structure transitions of the type crystallization–amorphisation–crystallization (C-A-C) and amorphisation–crystallization–amorphisation (A-C-A) are implemented

4. The CO_2-laser radiation with wavelength 10.6 μm can be used as a thermal probe discovering metastable phases fully in accordance with the Ostwald principle because of “laser” processing conditions; it is short-term and non-stationary heating.

5. A laser with another wavelength with sufficient degree of absorption is also suitable for material structure modification, which allows a volume modification of the structure for transparent materials.

Acknowledgements

Authors are grateful to E.B. Yakovlev and N.V. Nikonorov for useful discussions, to A.N. Rachinskaya for participation in some experimentation, to V. Ermakov for assistance in the process of Raman scattering spectroscopy, to A.I. Ignat'ev and R. Nuryev for assistance in XRD measurements and evaluation.

The study was supported by Russian State Contracts RSC № 14.B37.21.0144 and 16.740.11.0588, Russian Federation President Grant for leading scientific school SS–619.2012.2 and RFBR Grant 12–02–01194a.

References

[1] R.R Gattas and F. Mazur: Nature Photonics, 2, (2008) 219. (Journals)
[2] Y. Cheng, K. Sugioka and K. Midorikawa: Appl. Surf. Sci., 248, (2005) 172. (Journals)
[3] T.R. Dietrich, A. Freitag and R. Scholz: Chem. Eng. Technol, 28 (4), (2005) 1. (Journals)
[4] B. Fisette, F. Busque, J-Y. Degorce and M. Meunier: Appl. Phys. Lett., 88, (2006) 091104-1. (Journals)
[5] F.E. Livingston and H. Helvajian: "Photophysical processes that lead to ablation-free microfabrication in glass-ceramic materials" in "3D laser microfabrication. Principles and Applications" ed. by H. Misawa and S. Juodkazis (WILEY-VCH, Weinheim, 2006) p.403. (Books)
[6] S.K. Ahn, J.G. Kim, V. Perez-Mendez, S. Chang, K.H. Jackson, J.A. Kadyk, W.A. Wenzel and G. Cho: IEEE Trans. Nucl. Sci, 49, (2002) 870. (Journals)
[7] V.P. Veiko and K.K. Kieu: QUANTUM ELECTRON, 37 (1), (2007) 92. (Journals)
[8] V.P. Veiko, E.B. Yakovlev and E.A. Shakhno: QUANTUM ELECTRON, 39 (2), (2009) 185. (Journals)
[9] E.I. Ageev, V.P. Veiko and K. Khanh: Proc. SPIE, 7996, (2011) p.79960R-1. (Conference Proceedings)
[10] Y. Cheng, K. Sugioka and K. Midorikawa: Proc. SPIE, 5662, (2004) p.209. (Conference Proceedings)
[11] P.A. Skiba, V.P. Volkov, K.G. Predko and V.P. Veiko: Opt. Eng., 33 (11), (1994) 3572. (Journals)
[12] V.P. Veiko, G.K. Kostyuk, N.V. Nikonorov, A.N. Rachinskaya, E.B. Yakovlev and D.V. Orlov: SPIE, 6606, (2007) p.66060Q-1. (Conference Proceedings)
[13] M. Masuda, K. Sugioka, Y. Cheng, N. Aoki, M. Kawachi, K. Shihoyama, K. Toyoda, H. Helvajian and K. Midorikawa: Appl. Phys. A-Mater., 76, (2003) 857. (Journals)
[14] V.P. Veiko, G.K. Kostyuk, N.V. Nikonorov and E.B. Yakovlev: Bulletin of the Russian Academy of Sciences: Physics, 72 (2), (2008) 167. (Journals)
[15] S.M. Metev and V.P. Veiko: "Laser-assisted microtechnology" (Springer, Heidelberg, 1998) p.270. (Books)
[16] F.E. Livingston, P.M. Adams and H. Helvajian: Proc. SPIE, 5662, (2004) p.44. (Conference Proceedings)
[17] E.B. Yakovlev: "Features of behavior of glasses and glass-like materials at rapid heating" (SPb SUITMO, Saint Petersburg, 2004) p.88. (Books) [in Russian].
[18] V.P. Veiko, G.K. Kostyuk, N.V. Nikonorov and A.N. Rachinskaya: Bulletin of higher education institutions. Iinstrumentation, 49 (9), (2006) 5. (Journals) [in Russian].
[19] A.I. Berezhnoi: "Glass Ceramics and Photo-Sitalls" (Plenum Press, NY, 1970) p.444. (Books)

(Received: January 17, 2013, Accepted: April 24, 2013)